PHYSICAL REVIEW D, VOLUME 62, 081701(R)

Ground state in the Faddeev-Skyrme model

Jarmo Hietarinta*
Department of Physics, University of Turku, FIN-20014 Turku, Finland

Petri Salo
Helsinki Institute of Physics and Laboratory of Physics, Helsinki University of Technology, P.O. Box 1100, FIN-02015 HUT, Espoo, Finland

(Received 4 January 2000; published 18 September 2000)

New results are reported for the ground-state configurations of the Faddeev-Skyrme model. We started minimization runs on a large set of initial states and found topologically new ground states for the Hopf charges $Q=4$ and 5, and a symmetry-breaking deformation for $Q=6$. The corresponding energies improve the fit to the Vakulenko-Kapitanskii behavior $E\propto|Q|^{3/4}$.

PACS number(s): 11.27.+d, 11.10.Lm

The recent increased interest in knotted solitons with a nonzero Hopf charge is due to Faddeev and Niemi [1], who first suggested that Faddeev's Lagrangian [2]

$$L=\frac{1}{2}\int\left[(\partial_\mu\mathbf{n})^2+gF_{\mu\nu}^2\right]d^3x,$$

$$F_{\mu\nu}=\epsilon_{abc}n^a\partial_\mu n^b\partial_\nu n^c,\quad \mathbf{n}^2=1, \tag{1}$$

has stable ring-like solutions with the Hopf charge of 1 or 2. The Hopf charge characterizes the unit-vector field $\mathbf{n}$ as follows: the unit-vector field itself can be considered as a point on the sphere S^2, and furthermore, we assume that at spatial infinity all vectors point to the same direction and therefore we can compactify R^3 to S^3. The vector field then provides a map $\mathbf{n}:S^3\to S^2$, and since $\pi_3(S^2)=\mathbb{Z}$ these maps are classified by an integer Q, the Hopf charge.

The results for $Q=1,2$ in [1,3] were obtained under the assumption of rotational symmetry, but soon after results with full three-dimensional minimization were obtained in [4–6]. These results show that although the $Q=1,2$ cases may have rotational symmetry in the minimum energy state, this is not the case for higher charges. In [4] the starting point was a slightly perturbed ring un-knot with $Q=1-8$ and the following minimum configurations were found: $Q=1,2$ a rotationally symmetric ring; $Q=3,4,5$ a twisted ring; $Q=6$ two linked charge 2 rings; $Q=7$ a trefoil knot; $Q=8$ two doubly linked charge 2 rings. In [5] we started with linked un-knots of various charges and linking numbers. One difference between our results and those in [4] is that for $Q=4$ we obtained a different minimum configuration: two linked un-knots of charge 1 [5].

Soon after Faddeev proposed his model, Vakulenko and Kapitanskii (VK) obtained [7] (see also [8]) a lower bound for the energy of Eqs. (1) in the form

$$E\geqslant c\sqrt{g}|Q|^{\frac{3}{4}}, \tag{2}$$

where c is a constant, g is the coupling constant in (1), and Q is the Hopf charge. The comprehensive results of [4] follow the predicted Q dependence fairly well. However, for $Q=4$ and especially for $Q=5$ the value of the normalized energy $(E/|Q|^{3/4})$ obtained in [4] is noticeably higher than that for the other Q values. This raises a question about the true lowest energy state, especially since in [5] the minimum configuration is different for $Q=4$. One purpose of the present work is to clarify the question of the true minimum energy state.

Another open question is connected to the type of the ring configuration. Using the stereographic projection, the unit vector field can be represented in terms of a complex function U:

$$\mathbf{n}=\left(\frac{U+U^*}{1+|U|^2},-i\frac{U-U^*}{1+|U|^2},\frac{|U|^2-1}{1+|U|^2}\right),$$

where $U\to\infty$ as $\mathbf{r}\to\infty$. Let us now use toroidal coordinates η,ϕ,ξ defined by

$$x=a\frac{\sinh\eta\cos\phi}{\cosh\eta-\cos\xi},\quad y=a\frac{\sinh\eta\sin\phi}{\cosh\eta-\cos\xi},\quad z=a\frac{\sin\xi}{\cosh\eta-\cos\xi},$$

where ϕ is the angle around the z axis, ξ the angle around the torus ring (located at $z=0$, $x^2+y^2=a^2$), and η the distance from the ring. Un-knot vector fields are then obtained, e.g., with $U=f(\eta)e^{i(m\xi+n\phi)}$, which yields

$$\mathbf{n}=\left[\frac{2f}{f^2+1}\cos(m\xi+n\phi),\frac{2f}{f^2+1}\sin(m\xi+n\phi),\frac{f^2-1}{f^2+1}\right], \tag{3}$$

where it is assumed that $f(\eta)\to\infty$ as $\eta\to0$ and $f(\eta)\to0$ as $\eta\to\infty$. The Hopf charge corresponding to such a configuration will be $Q=-nm$ [9]. In previous studies it has always been assumed that $|m|=1$ above, and we also wanted to know if lower energy configurations could be obtained with $|m|>1$.

Here we report new results obtained with (i) further continuing minimization on our previously obtained configura-

*Also at the Helsinki Institute of Physics.

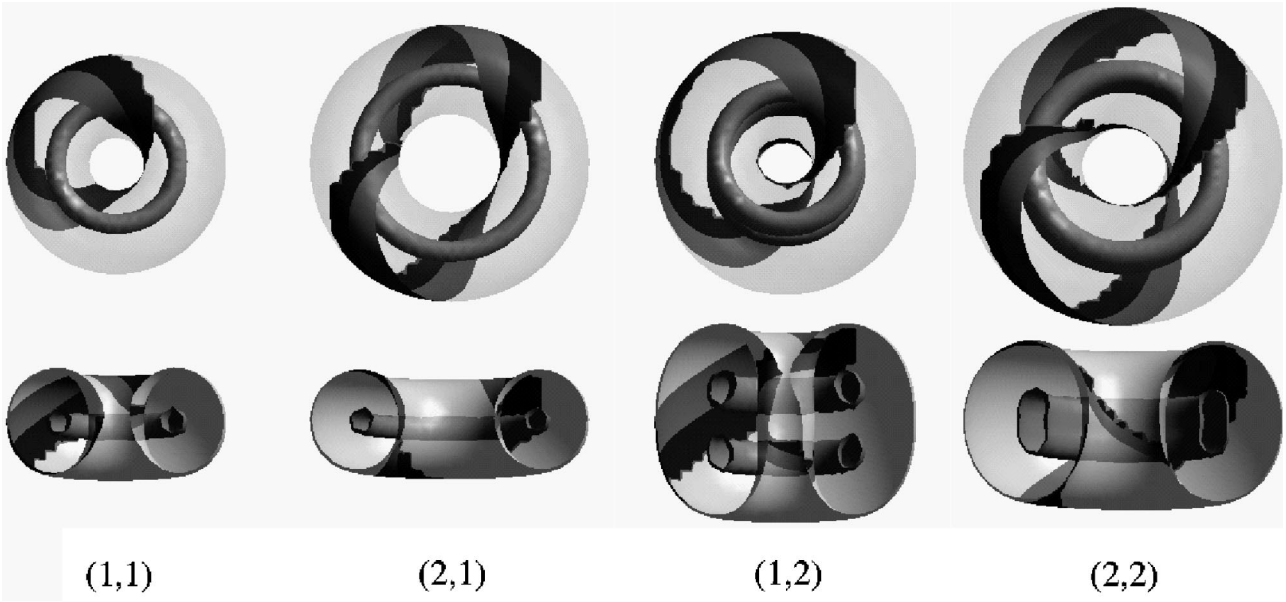

FIG. 1. The final configurations for (n,m) with $1 \leqslant |n|,|m| \leqslant 2$. The top view and the cut-out side view show the m inner ring(s) (isosurface $n_3 = -0.9$) and the transparent $n_3 = 0$ larger ring. The dark band on the $n_3 = 0$ isosurface is where the vector points to a particular fixed direction (perpendicular to the vacuum direction).

tions for $Q = 4,6$ and (ii) new minimization on the linked configurations $1+2+2$ and $1+3+2$, and on configurations with $|m| > 1$ in Eq. (3).

The minimum energy configurations were obtained numerically using the steepest descent method, which was improved by also taking into account the gradients of the previous step. The system was discretized on the cubic lattice; for details see [5]. In order to avoid singularities created by the stereographic projection we used the unit-vector field **n** itself (we normalized $|\mathbf{n}| = 1$ after each iteration step). The boundaries of the lattice were fixed to the vacuum value $\mathbf{n} = (0,0,1)$. For g we used the value 0.125. The fact that the system is discretized and put into a box with fixed boundaries introduces some errors to the energy and we will return to this question below. Our initialization method, also described in [5], enables us to make almost any kind of linked configuration.

The size of the grid was 120^3 or 240^3 depending on how large the gradients of the vector field **n** were. Whenever any nearest-neighbor vectors in the lattice differed by an angle of more than 30° in the sparser grid we put the system into the denser grid to ensure that no topology breakup occurred. The present computations were done on a Cray T3E parallel supercomputer. Each round of iteration took about two seconds for the 120^3 and 240^3 grid with 8 and 64 processors, respectively.

The total number of iterations was typically between 100 000 and 200 000 for $Q \geqslant 4$. The computations were terminated when we could see that the result was close enough to a known final state (similar isosurfaces and energy within 0.25% from the best result), or the minimization satisfied the convergence criterion. Previously we used the criterion of the order 10^{-7} per iteration for the relative change in energy, but this was apparently too lax, and for the present results we stopped the minimization only after the change was of the order 10^{-9}.

The stability of the final configuration was tested by disturbing it and then checking if it evolved back to its original configuration or to another, lower minimum configuration. For this purpose the most efficient Hopf charge preserving jolt was a 1:2 squeeze along some direction, but we also tried stretching, especially in initial configurations, and also random force. In some cases we could not get out of the local minimum with any such method, which indicates that the configuration was at a stable local minimum.

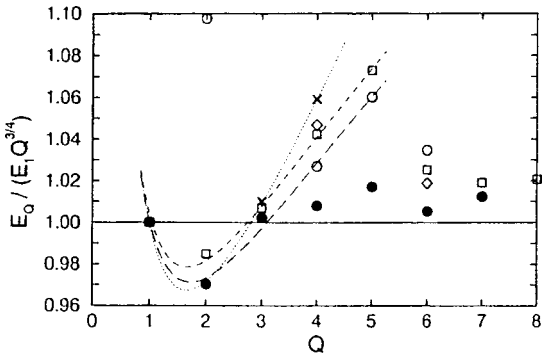

FIG. 2. Normalized energies for different configurations vs Hopf charge Q. Filled circles represent our global minima for $Q = 1-7$, open circles our local minima $(Q = 2,4,5,6)$, diamonds our previous local minima [5] for $Q = 4$ and 6, crosses our rotationally symmetric local minima $(Q = 3,4)$, and open squares the global minima [4] for $Q = 1-8$. The long-dashed line is a linear fit to our bent rings $Q = 1-5$, the dashed line a linear fit to $Q = 1-5$ of [4], and the dotted line a quadratic fit to our symmetric rings $Q = 1-4$. The horizontal line represents the $Q^{3/4}$ behavior.

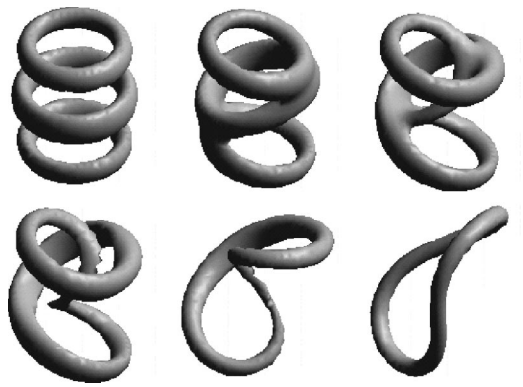

FIG. 3. Deformation of (1,3) into (3,1). We display a small tube (defined by the isosurfaces $n_3=-0.875$) around the core $n_3=-1$.

To indicate the form of the initial configuration we use the notation (n,m) for any un-knot topologically identical to Eq. (3). For $1\leqslant|n|,|m|\leqslant 2$ the final configuration differs from the initial one only slightly; in particular the rotational symmetry seems to be preserved. Figure 1 shows the final states for these low (n,m) cases. We can see that m counts the number of times the vector field turns when we go around the small circle of the torus, while n counts the turns around the large circle. If $|m|=2$ the initial vector field looks like a dipole field around the ring; in the final state this dipole is split into two rings on top of each other.

In Fig. 2 we present the normalized minimum energies $E_Q^*=E_Q/(E_1Q^{3/4})$. We will discuss the figure in detail below; here we just want to point out that for $Q=2$ the conventional (2,1) case is below the standard level, while (1,2), which seems to be a local minimum, is far above (the open circle at 1.098).

TABLE I. All initial configurations listed together with the final state, its shape (symmetric, bent, linked, knotted) and its energy. An asterisk star means that the system first relaxed into a metastable state and the final state was obtained only after the minimization was restarted from a modified (topologically identical) state.

$\|Q\|$	initial	final	form	E_Q
1	(1,1)	(1,1)	symm	135.2
2	(2,1)	(2,1)	symm	220.6
	(1,2)	(1,2)	symm	249.6
3	(3,1)*, (1,3)	(3,1)	bent	308.9
	(3,1)	(3,1)	symm	311.3
4	(2,2), 1+1+2	(2,2)	symm	385.5
	(4,1)*,(1,4)	(4,1)	bent	392.7
	(4,1)	(4,1)	symm	405.0
5	(5,1)*, (1,5), 1+2+2	1+2+2	link	459.8
	(5,1)	(5,1)	bent	479.2
6	2+2+2*, (3,2)	2+2+2	link	521.0
	1+3+2, (1,6), (2,3)	1+3+2	link	536.2
7	4+5−2, (7,1)*, (1,7)	trefoil	knot	589.0

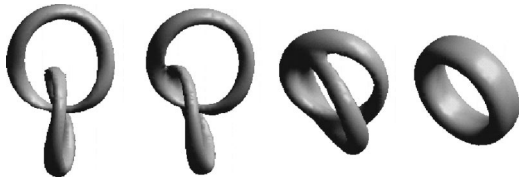

FIG. 4. Deformation of $1+1+2$ into (2,2). (Isosurfaces $n_3=-0.85$).

None of the other configurations with $|m|>1$ were stable. As an example we give in Fig. 3 the steps by which the initial (1,3) un-knot deforms into the (3,1) bent ring found in [4]. We did similar studies for $(1,m)$ up to $m=7$, as well as (2,3) and (3,2). Usually the process was as in Fig. 3: the multipole inner ring opens into multiple rings which connect, forming a single ring, which then twists and reconnects further into the usual final configuration. The results are collected in Table I.

In addition to these new configurations we studied further the state of the previously obtained minima. As noted before, the $Q=4,5$ energies reported in [4] deviate noticeably from the best fit VK bound (2). Our best result for $Q=4$ in [5] was obtained by a linked $1+1+2$, but when we continued the minimization further we found that the rather symmetric $1+1+2$ configuration slowly developed some asymmetry and then quickly deformed into a (2,2) configuration, which has a still considerably lower energy. Some steps in this sequence are shown in Fig. 4. Thus in some cases the local minimum is more like a very gentle slope or terrace where the system stays a long time until it starts to evolve toward a lower minimum.

For $Q=5$ the minimum configuration reported in [4] was a bent ring. However, we have now found that the linked configuration $1+2+2$ has a much smaller energy. The charge 5 bent ring is apparently a metastable local minimum, and indeed, after squeezing, it deformed into a $1+2+2$ linked configuration, shown in Fig. 5. This same configuration also followed when we started from the initial state (1,5).

For $Q=6$ we tried several initial states, (1,6), (2,3), (3,2), $1+3+2$, and we also continued from the previously obtained $2+2+2$. All initial configurations relaxed into either $1+3+2$ or $2+2+2$ (see Table I). We used squeezing

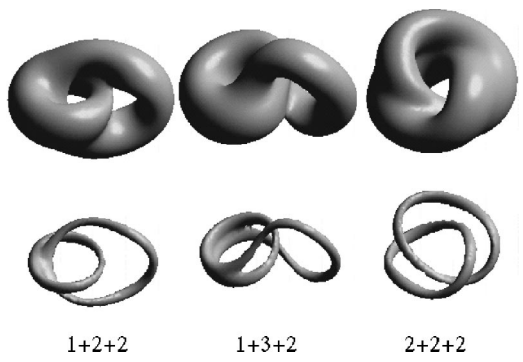

FIG. 5. Final states for $1+2+2$, $1+3+2$, and $2+2+2$. (Isosurfaces $n_3=0$ and $n_3=-0.9$.)

in order to get out of the previously obtained $2+2+2$ symmetric local minimum, and then the system deformed into a butterfly-shape $2+2+2$ structure (see Fig. 5) with a somewhat lower energy. This is also the final configuration obtained from (3,2). Several other initial states relaxed into $1+3+2$, which apparently is a local minimum with a higher energy than that of $2+2+2$. It is interesting that for $1+3+2$ the rings are not clearly separated, but almost glued to each other at one point.

We have also studied some more complicated systems with linked un-knots (with low total Hopf charge), and it turned out that the linked configuration of (n_1,m_1) and (n_2,m_2) always deformed into one of the previously found configurations with the Hopf charge $-n_1m_1-n_2m_2+2m_1m_2$. Further details will be reported elsewhere.

Let us now return to Fig. 2, which gives the normalized energies. Our best minima (filled circles for $Q=3-7$ in Fig. 2) seem to fit well into the predicted $E\propto Q^{3/4}$ behavior. In particular the fit reported in [4] is considerably improved with the new minimum configurations for $Q=4$: (2,2) and $Q=5$: $1+2+2$. The slightly asymmetric deformation obtained for $Q=6$ improves the fit as well.

The energies of the mostly metastable bent rings (symmetric for $Q=1,2$ and bent for $Q=3-5$; see also Table I) turn out to be well described by a linear fit $(E_Q/E_1=0.36+0.64Q)$ proposed recently [10]. A similar fit $(0.36+0.65Q)$ works for the energies of the bent configurations for $Q=1-5$ given in [4]. (In Fig. 2 the dashed lines appear curved because we have plotted E^* which contains a $Q^{-3/4}$ factor.) It should be noted, however, that the linear fit is good only if it is limited to the bent un-knots. For the energies of the rotationally symmetric un-knots, which are reported here and those given in [4], a small quadratic term improves the fit further $(0.39+0.59Q+0.015Q^2$, dotted line).

The absolute energies can be compared after the different choices for coupling constants are taken into account [cf. (2)]. For this purpose we can use the parameter K_0 proposed by Ward [8]. In our case $K_0=111.7$ and we find that $E_Q/(Q^{3/4}K_0)=1.21-1.23$, except that for $Q=2$ we get 1.17. This is in good agreement with the results of [3] and supports Ward's conjecture that the soliton energies are about 20% higher than the bound K_0.

We have also studied the systematic error related to boundary pressure and discretization. In order to study the boundary effects we embedded every final global minimum configuration calculated with a 120^3 lattice into the center of a 240^3 lattice and allowed it to relax there. Similarly, the discretization effects were studied by making the grid twice as dense. The results show that putting the boundaries further away decreases the energy by 0–0.5% while doubling the discretization increases the energy by 1.2–1.8%. Since these trends are the same for all configurations the relative error of the normalized energies is quite small, and thus the energies for different configurations can be compared with each other.

In summary, we have reported new results for the ground-state configurations of the Faddeev-Skyrme model, in particular topologically new ground states for $Q=4$ and 5. With these new results the energy can be seen to follow quite nicely the $Q^{3/4}$ law. It would now be interesting to find an explanation for the anomalously low energy for charge $Q=2$. Another open question is the full characterization of the vector-field deformation process.

ACKNOWLEDGMENTS

We would like to thank L. Faddeev, A. Niemi, P. Sutcliffe, and W. Zakrzewski for discussions and M. Gröhn, J. Pirhonen, and J. Ruokolainen for help in the visualization aspects of this work. We are grateful to the Center for Scientific Computing, Espoo, for computer time on the Cray T3E parallel machine, where most of the computations reported here were made.

[1] L. Faddeev and A. Niemi, Nature (London) **387**, 1 (1997); hep-th/9705176.

[2] L. Faddeev, IAS Print 75-QS70 (1975); L. Faddeev, in *Relativity, Quanta, and Cosmology*, edited by M. Pantaleo and F. De Finis (Johnson, New York, 1979), Vol. 1, pp. 247–266.

[3] J. Gladikowski and M. Hellmund, Phys. Rev. D **56**, 5194 (1997).

[4] R. A. Battye and P. M. Sutcliffe, Phys. Rev. Lett. **81**, 4798 (1998); Proc. R. Soc. London **A455**, 4305 (1999).

[5] J. Hietarinta and P. Salo, Phys. Lett. B **451**, 60 (1999).

[6] Relevant video animation can be seen at `http://users.utu.fi/hietarin/knots`

[7] A. F. Vakulenko and L. V. Kapitanskii, Sov. Phys. Dokl. **24**, 433 (1979).

[8] R. S. Ward, Nonlinearity **12**, 241 (1999).

[9] H. Aratyn, L. A. Ferreira, and A. H. Zimerman, Phys. Rev. Lett. **83**, 1723 (1999).

[10] M. Miettinen, A. Niemi, and Y. Stroganov, Phys. Lett. B **474**, 303 (2000).